SEPTEMBER 1980 LA. 1787 PPPL-1696
UC-20f

NEUTRON FLUX MEASUREMENTS AROUND PLT

BY

G. ZANKL, J. D. STRACHAN, R. LEWIS,
W. PETTUS, AND J. SCHMOTZER

PLASMA PHYSICS LABORATORY

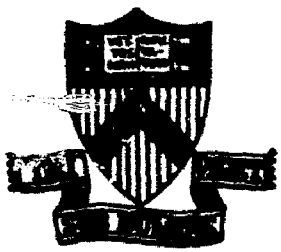

PRINCETON UNIVERSITY
PRINCETON, NEW JERSEY

This work was supported by the U.S. Department of Energy Contract No. DE-AC02-76-CHO 3073. Reproduction, translation, publication, use and disposal, in whole or in part, by or for the United States

Neutron Flux Measurements Around PLT

G. Zankl* and J. D. Strachan

Plasma Physics Laboratory, Princeton University

Princeton, New Jersey 08544

R. Lewis, W. Pettus, and J. Schmotzer

Babcock & Wilcox

Lynchburg, Virginia 24505

ABSTRACT

Using Indium activation foils, the toroidal and poloidal neutron emission patterns were determined for PLT plasmas which include ICRF and neutral beam heating. The activities produced by the ^{115}In (n,n') ^{115m}In reaction were determined by counting the 336 keV γ line of the ^{115m}In decay. This activation cross section falls just below 2.5 MeV so that the influence of scattered neutrons of degraded energies is reduced. From the magnitude of the activity, the absolute calibration of the PLT fusion neutron emission is obtained with $\lesssim$ 40% accuracy.

* on leave from Max-Planck Institut für Plasmaphysik

INTRODUCTION

The neutron emission from the PLT plasma consists primarily of 2.5 MeV neutrons produced by $d(d,n)^3He$ fusion reactions. The large, extended nature of the plasma and the massive scattering centers located near the plasma mean that the local neutron flux and energy distribution is spatially complex. Consequently, the spatial resolution of the neutron emission inside the plasma and the absolute calibration of the neutron emission are difficult measurements to perform. The eventual design of blanket modules around a tokamak reactor[1] will also require accurate, local, neutron energy and flux measurements.

In this paper, we describe the first measurements of the spatial symmetry of the energetic neutron flux around a tokamak. The measurement is performed using Indium activation[2] foils which are mounted around PLT for a discharge series (lasting up to 5 hours) and which are subsequently analyzed for neutron induced activity. Indium is particularly well-suited as an activation detector for 2.5 MeV neutrons since the $^{115}In\ (n,n')\ ^{115m}In$ is a threshold reaction whose cross section falls just below a neutron energy of 2.5 MeV. Activation by scattered neutrons is therefore reduced since these neutrons suffer an energy loss in the elastic and inelastic scattering processes. However, we have found that $^{115}In\ (\gamma,\gamma')$ reactions can also occur when the foils are used near the PLT limiters. The energetic photons ($\geq$ 10 MeV) originate from runaway electron bombardment of the limiter.[3] By careful monitoring of other Indium photo-reactions induced in the foil, we could identify photo-activated foils, and thereby avoid spurious ^{115m}In activation by not using such foils.

The neutron activated Indium foils were useful in establishing that the PLT neutron emission was toroidally uniform during ICRF and neutral beam heating. In particular, there was no enhanced emission in the vicinity of the ICRF coils. We were able to discern an outward shift in the neutron emitting region during neutral beam heating that is consistent with the Shafranov shift of the central plasma column. The foils provide an accurate, absolute neutron calibration which is inexpensive and easy to accomplish.

INDIUM ACTIVATION REACTIONS

The foils used in our experiments are composed of Indium in its natural isotopic concentration (95.7% ^{115}In and 4.3% ^{113}In). The radioactivity induced by the PLT discharges is listed in Table I and originates from either photon or neutron induced reactions. The radioactivity is identified by measurement of the γ emission unique to each decaying radionuclide (Table II). The γ- spectra were measured with a high resolution Ge(Li) detector and were found to fall into two distinct spectral types (Fig. 1, Table II). The type N spectra were obtained on PLT discharges with low levels of runaway electrons and high levels of 2.5 MeV fusion neutron emission resulting from neutral beam or ICRF heating. The type P spectra were obtained on PLT discharges with large levels of runaway electrons when the foils were located near the PLT limiter in the forward cone of hard x-radiation induced by the runaway electrons encountering the PLT limiters.

We are primarily interested in the $^{115}In(n,n')\ ^{115m}In$ threshold reaction since its cross section[4] has a maximum at about the energy of the 2.5 MeV fusion neutron (Fig. 2). Due to the nature of this cross section, activation by scattered neutrons is of reduced importance since the scattering process reduces the neutron's energy.

One fundamental problem with this reaction is that the final ^{115m}In state can also be achieved by the runaway electron induced $^{115}In(\gamma,\gamma')$ ^{115m}In reaction[5] (Fig. 3, Table I). In the use of the Indium foils, we have avoided ^{115m}In (γ,γ') activation by a) limiting the use of foils to regions away from the limiters, b) limiting the use of foils to discharges which do not include disruptions, or large runaway electron levels, and c) restricting our analysis to foils with type N spectra. We believe that the lack of any of the photo-induced ^{114}In, ^{112}In, ^{112m}In, or ^{111m}In nuclides of the P type γ spectra effectively discriminates against complications due to $^{115}In(\gamma,\gamma')$ activity. About 10 cm of wax was placed between the plasma and the In foils, resulting in > 10x reduction of the ^{115m}In activity. This indicates that type N, ^{115m}In activation is due primarily to neutrons and not photons since the energetic photons would be attenuated by only 20%.

Another problem is the room background ^{228}Ac radioactivity which produces ~.06 counts/s in the Ge(Li) detector at 0.338 MeV. This background line interferes with the observation of the ^{115m}In, 0.336 MeV γ line (Fig. 4) unless the ^{115m}In activity is sufficiently large. Discrimination against this background line and counting statistics (taking into account the background counts) leads to a minimum usable 0.336 MeV γ count rate of 0.02 counts/s. which can be resolved with an error ~50%. This means that the minimum 2.5 MeV neutron flux that can be resolved with a 10 g In foil is $\sim 10^6$ n/cm^2. Therefore, a foil mounted on the PLT vacuum vessel produces a measurable ^{115m}In activity for total doses $\gtrsim 2.5 \times 10^{11}$ neutrons which should be produced roughly within the 4.4 hour ^{115}In half life.

Another useful Indium reaction is $^{115}In(n,\gamma)^{116}In$ which gives qualitative information on the component of low energy neutrons present at any location. Use of a 0.5 mm Cadmium around the Indium provides a thermal neutron shield

which means that this ^{116}In activity level is most sensitive to the local flux of 1 eV neutrons. The dotted lines in Fig. 2 represent the effective ^{115}In (n,γ) cross section in the low energy range when the Cadmium shield is in place. The ratio of the ^{115}In (n,γ)/^{115}In(n,n') cross sections at 2.5 MeV indicates that an activity ratio of $^{116}In/^{115m}In$ ~0.2 would be obtained for a pure 2.5 MeV neutron field. Typically at the PLT vacuum vessel, we observed $^{116}In/^{115m}In$ ≈ 20 for type N spectra. A 1 eV scattered neutron flux of $\sim 10^{-2}$ of the energetic 2.5 MeV neutron flux is sufficient to produce the observed ^{116}In activity.

LOCAL NEUTRON FLUX MEASUREMENTS

The local neutron flux, Γ_n (n/cm^2), produces a specific activity in the foils A* (disintegrations/s). The specific activity is determined simply from the mass of the foil (~10g), the efficiency of the Ge(Li) detector for disk-shaped samples at the energy of the observed γ radiation (~5.4% at 0.336 MeV), the amount of emitted γ-rays per disintegration and a correction factor for γ self-absorption in the activation foil (0.96). The principal uncertainties in determining the local flux from the specific activity are cross section uncertainties (± 5%), and counting statistics.

$$A_o^* = \frac{c_o}{ma\varepsilon\alpha\beta} \qquad (1)$$

where A_o^* = specific activity at time t_o,

c_c = the count rate at time t_o,

m = mass of the probe (~10g),

a = abundancy of the isotope (0.957 for ^{115}In),

ε = efficiency of the Ge(Li) detector for disk-shaped foils at the energy of the observed γ (5.4% at 0.336 MeV),

β = factor for γ self-absorption in the activation foil (0.96),

α = γ counts per disintegration (0.459).

The neutron flux, Γ_n (n/cm^2) producing a specific activity, A_{o*}, is

$$\Gamma_n = \frac{A\, A_o^*}{\lambda \sigma N_L} = 1.298 \times 10^7\, A_o^* , \qquad (2)$$

where A = atomic mass of the initial nuclide,

σ = the activation cross section,

λ = decay constant of the nuclide produced,

and N_L = Avogadro's number.

We have measured the local 2.5 MeV and 1 eV neutron fluxes at a number of PLT positions. We found that the flux was toroidally symmetric (Fig. 5) during either neutral beam heated ($D^o \rightarrow H^+$, or $H^o \rightarrow D^+$) ohmic heated, or ICRF heated (^3He minority, or d minority) PLT discharges. This measurement is particularly useful for rf heated discharges,[6] where near field ion acceleration could lead to enhanced neutron emission in the vicinity of the rf coils.

We found that the 1 eV scattered neutron flux was about 10^{-2} of the 2.5 MeV primary neutron flux at the vacuum vessel. About 75 cm away from the

vacuum vessel, the 2.5 MeV flux had fallen to 1/5 while the 1 eV flux had fallen to 1/3 (Fig. 6). An Indium foil located on the back of a copper toroidal magnetic field coil (Fig. 7) sees a 2.5 MeV neutron flux about 1/50 of a foil places on the vacuum vessel although the 1 eV neutron flux has fallen only ~1/3. Evidently, positions further away from the plasma have a larger contribution of scattered neutrons in the local flux.

We found that there could be a small poloidal asymmetry to the neutron emission (Fig. 8) whereby the local flux at the outside horizontal midplane is enhanced. The poloidal symmetry is particularly sensitive to major radial displacements of the central plasma column. We found for $D^{o}\rightarrow H^{+}$ neut. al beam injection (2Co + 1CTR) that the neutron emitting region was outshifted about 8 cm from the vacuum vessel center and downshifted by about 1 cm. This outward plasma column shift was also observed on the soft X-ray emission from the plasma when viewed vertically (Fig. 9) and is consistent with the expected central Shafranov shift of the plasma column plus the energetic Co ion drift orbit displacement.[7]

Without scattering, the neutron flux at a distance r_f from a toroidal line source and at a poloidal angle θ (Fig. 10) is

$$\Gamma_n = \frac{N}{2\pi^2 r_f} \frac{\arctan \dfrac{\left(4R^2 + r_f^2 + 4r_f R\cos\theta\right)^{1/2} \tan\left(\phi_o/2\right)}{r_f}}{\left(4R^2 + r_f^{\,2} + 4r_f R\cos\theta\right)^{1/2}} \quad , \quad (3)$$

where N is the total neutron yield,

R is the toroidal major radius, and

ϕ_o is a toroidal cutoff angle as determined by massive obstructions such as the PLT center column or toroidal field coils. Equation (3) can reasonably explain the local flux of 2.5 MeV neutrons so long as neutron attenuation by the toroidal magnetic field coils (Figs. 6 and 7) is used to determine ϕ_o at large r_f. The toroidal major radius, R, strongly influences the poloidal symmetry (Fig. 9).

ABSOLUTE NEUTRON CALIBRATION

As there is some decay of activation during the exposure, the total neutron emission, N_o, is determined from the individual PLT discharges

$$N_o = \sum_i N_i e^{-\lambda (t_o - t_i)} , \qquad (4)$$

where N_i = the neutron emission of one pulse i,

t_i = time of pulse i,

t_o = time of the last pulse.

For example, the neutron emission from 109 PLT discharges within a total time of 6 hours (Fig. 11) having an average neutron emission ~5 x 10^{12} sec^{-1} for ~0.1 sec is equivalent to a total activation due to 3.7 x 10^{13} neutrons if the entire neutron irradiation had occurred at the time of the last PLT discharge.

The major difficulty in utilizing Eq. (3) to absolutely calibrate the neutron emission is the difficulty in assessing the influence of absorption and scattering on the local neutron flux. This is true of any method for determining the absolute neutron emission; however the use of the Indium foils has potential advantages of favorable locations and a favorable cross section for reducing the influence of scattered neutrons. Elastic scattering from materials with large atomic weights (e.g., Fe, Ni, and Cu) cause a relatively small change in the neutron energy so that such scattered neutrons will still have a reasonable probability of inducing $^{115}In(n,n')$ reactions. Elastic scattering from materials with low atomic weights (especially hydrogen) as well as inelastic scattering effects cause relatively larger changes in the neutron energy so that such scattered neutrons will have a reasonably small probability of inducing $^{115}In(n,n')$ reactions. The epoxy used in binding the toroidal field, ohmic heating, and equilibrium field windings has a high hydrogen content and is quite effective at reducing the neutron energy so that these scattered neutrons do not induce $^{115}In(n,n')$ reactions. The position of the foil on the vacuum vessel means that back scatter from copper coils and forward scatter from the vacuum vessel are the most important effects.

Estimating the activation caused by scattered neutrons indicates that the total activation should be 1.24 ± 15% (Table III) of the activation induced by the primary neutrons. These estimates are based on reflection and transmission experiments using PuBe neutron source. The In(n,n') activation increased by a factor of 1.03 ± 5% upon transmission through a piece of vacuum vessel. A reduction in the Indium activity of 5% is expected due to inelastic scattering. However the elastic scattering changes the angular distribution of the incident neutrons causing the scattered neutrons to have longer mean path lengths through the foils and thus leading to a net increase of the total activation.

The reflection coefficient for neutrons to backscatter off toroidal field coils and ohmic heating coils was determined by measuring the increase in PuBe activation when a coil was immediately behind the foil. The activity increased by a factor of 1.15 due to the combined scattering from the poxy-casted copper coils. The calculated increases in activity (Table III) were obtained by integrating the scattered flux returning to the foil along the various machine components and multiplying by the reflection coefficient. Since the PuBe neutrons are more energetic than 2.5 MeV we expect that the calculated activation enhancement of 1.24 is an overestimate.

In addition, we have measured the neutron spectrum with a collimated ^{3}He ionization chamber which was situated about 5m from the plasma. The neutron spectrum (Fig. 12) indicates about as many neutrons with significantly degraded energies (i.e., 1→2.4 MeV) as neutrons with energies not significantly degraded from 2.5 MeV. Based on the observed spectrum, the neutrons below 2.4 MeV would contribute about 40% of the $^{115m}In(n,n')$ activation of an In foil placed inside the neutron collimator. This contribution due to obviously scattered neutrons is larger than the 20% contribution expected for the In foils on the vacuum vessel. We expect that scattering from the many material obstacles in the 5m neutron flight path to the collimated detector might account for the larger scattered contribution.

The largest source of error in the absolute neutron calibration is the neutron scattering which we quote as being uncertain to 15→40% based upon the calculation of the scattering contribution (Table III) and the neutron spectrum determination of the scattering (Fig. 12). The remaining important uncertainties (Table IV) are in relating the specific activity to the local flux [Eqs. (1) and (2)]. The cross section for the $^{115}In(n,n')$ activation is known to ± 5%. We estimate an uncertainty in the determination of the Ge(Li)

detector efficiency for the 336 keV γ line to be ± 5%. The statistical error due to the γ-counting was kept below 1%. We know the major radius of the neutron emitting zone from the poloidal symmetry of the neutron emission (Fig. 8) to be within ± 2 cm leading to a calibration error of ± 4%. The choice of the cut-off angle for the absorption of neutrons by the central structure of the device is not very sensitive. A ± 10% uncertainty for this angle leads to a ± 1% error in the calibration. The fact that the neutron source has a radial profile of about 30 cm FWHM adds an error of about 2%.

The absolute calibration so determined by the activation of the Indium foils compares reasonably with other methods of calibrating the PLT neutron emission.[9] The Indium foil method is, however, simpler to use, inexpensive, and more accurate. The magnitude of the neutron emission so calibrated agrees with the expected thermonuclear neutron emission for PLT ohmic heated deuterium discharges to within the uncertainties that this neutron emission can be calculated.[10] The magnitude of the calibrated neutron emission also agrees with the expected beam-target neutron emission during $D^{O} \rightarrow D^{+}$ neutral beam injection.[9,11] The use of the Indium calibration removes one of the primary uncertainties in the comparison of beam induced neutron emission with theory.[12]

ACKNOWLEDGMENTS

The authors thank W. Stodiek and the PLT group, H. Eubank and the neutral beam injection group, J. Hosea and the ICRF group, as well as J. Stencel who supplied the Ge(Li) detector for help in performing these measurements. Helpful discussions with R. Goldston, D. Jassby, and N. Sauthoff, are gratefully acknowledged. Technical and computational assistance in performing

the measurements was supplied by G. Estepp and J. Hovey. This work was supported by the U.S. Department of Energy Contract No. DE-AC02-76-CH03073.

REFERENCES

1. L. Kuijers et al., Nucl. Instr. & Meth. 144 (1977) 215.
2. K. H. Bechurts and K. Wirtz, "Neutron Physics" Springer-Verlag, New York (1964).
3. J. D. Strachan et al., Nucl. Fus. 17 (1977) 140.
4. H. Liskien et al., Nucl. Sci. and Eng. 67 (1978) 334.
5. O. V. Bogdamkevick, L. E. Lazarena, and F. A. Nikolaev, Sos. Phys., JETP 4 (1957) 320, J. Goldenberg, and L. Katz, Phys. Rev. 90(1953) 308; J. L. Burkhardt, E. J. Winhold, and T. H. Dupree Phys. Rev. 100 (1955) 199.
6. J. Hosea et al., Proc. 8th Int. Conf. on Plasma Phys. and Contr. Nucl. Fus. Research, Brussels (1980) paper IAEA-CN-38/D-5-1.
7. L. A. Artsimovitch, Nucl. Fus. 12 (1972) 215.
8. J. D. Strachan et al., Nature 279 (1979) 626.
9. P. Colestock et al., PPL-TM-325 (1979); P. Colestock et al., Proc. 9th European Conf. on Contr. Fusion and Plasma Phys, 1, 45 (1979) (Oxford).
10. M. Brusati et al., Nucl. Fusion 18 (1978) 1205.
11. H. Eubank et al., Phys. Rev. Lett. 43 (1979) 270.
12. J. D. Strachan et al., "Joint Varenna-Grenoble International Symposium on Heating in Toroidal Plasmas", Vol. 1, (Grenoble, 1978) 25.

TABLE I

INDIUM ACTIVATION SCHEMES

Initial Nucleus	Reaction	Cross-Section (b)	at Energy	Decay Scheme	Final Nucleus
^{115}In	(n,γ)	10^{4}	1 eV	$^{116m_2}In(2s) \xrightarrow{IT} {}^{116m_1}In(54m) \xrightarrow{\beta^-,\ \gamma = 1294, \text{etc}}$	^{116}Sn
		10^{-1}	2.5 MeV		
^{115}In	(n,n')	.343	2.5 MeV	$^{115m}In(4.49h) \xrightarrow{\beta^-}$ / $\xrightarrow{IT,\ \gamma = 336}$	^{115}Sn
	(γ,γ')	$\sim 2 \times 10^{-3}$	8 MeV		^{115}In
^{115}In	(n,2n)	1.5	14 MeV	$^{114m}In(49.5d) \xrightarrow{EC}$ / $\xrightarrow{IT,\ \gamma=191} {}^{114}In(72s) \xrightarrow{EC,\ \beta^-}$	^{114}Cd
	(γ,n)	.2	14 MeV		
^{113}In	(n,γ)	$\sim 10^{4}$	1 eV		^{114}Sn
^{115}In	(γ,2n)	.06	20 MeV	$^{113m}In(99.5m) \xrightarrow{IT,\ \gamma = 392}$	^{113}In
^{113}In	(n,n')	.2	2.5 MeV		
^{113}In	(n,2n)	1.5	14 MeV	$^{112m}In(21m) \xrightarrow{IT,\ \gamma=156} {}^{112}In(14.4m) \xrightarrow{EC,\ \beta^+,\ \gamma=511,617}$ / $\xrightarrow{\beta^-}$	^{112}Cd
	(γ,n)	.2	14 MeV		^{112}Cd
^{113}In	(γ,2n)	.06	20 MeV	$^{111m}In(7.6m) \xrightarrow{IT,\ \gamma=537} {}^{111}In(2.8d) \xrightarrow{EC} {}^{111m}Cd(49m) \xrightarrow{IT}$	^{111}Cd

TABLE II

INDIUM γ SPECTRA

Nuclide	Half Life	γ-line (keV)	γ/dis	Typical N Spectra (cps)	Countrates P Spectra (cps)
$^{116m}_{49}In$	54.3m	138	0.028	6.36	0.70
		355	0.007	0.21	---
		417	0.235	21.57	2.65
		463	0.007	0.41	0.08
		818	0.109	4.34	0.53
		1097	0.543	17.66	2.17
		1293	0.800	21.69	2.52
$^{115m}_{49}In$	4.49h	336	0.459	8.49	7.25
$^{114m}_{49}In$	49.5d	191	0.17	---	0.35
		558	0.03	---	0.02
$^{113m}_{49}In$	99.5m	392	0.64	0.57	1.33
$^{112m}_{49}In$	20.9m	156	0.13	---	3.21
$^{112}_{49}In$	14.4m	511	0.655	---	7.27
		617	0.060	---	0.54
$^{111m}_{49}In$	7.6m	537	0.87	---	0.02

TABLE III

ABSORPTION AND SCATTERING EFFECTS

Object of Absorption and Scattering	Change of Activity	Uncertainty
Wall of Vessel	1.030	± 5.0%
Inner Structure	1.028	± 1.5%
TF Coils	1.038	± 2.0%
OH Coils	1.072	± 1.5%
Other Equipment	1.050	± 5.0%
Total	1.24	± 15%

TABLE IV

Uncertainties in the Neutron Calibration

Sources of Uncertaintes:	Uncertainty Contributions
Cross Section for $^{115}In(n,n')^{115m}In$	± 5%
Detector Efficiency	± 5%
Counting Statistics	± 1%
Major Radius Uncertainty (± 2 cm)	± 4%
Cut Off Angle for Absorption by the Center Column ± 10^{o}	± 1%
Extended Neutron Source	± 1%
Absorption and Scattering	± 15-40%
Total:	± 18-45%

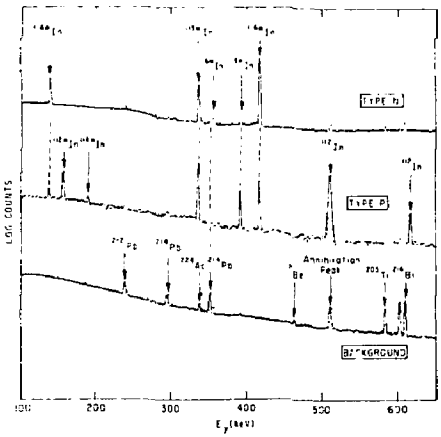

(PPPL-806099)

Fig. 1. Ge(Li) γ-spectra of the radioactive decays from PLT irradiated Indium foils. The type N spectrum is from the fusion neutron irradiated foil. The type P spectrum is from the photon irradiated foil. The background spectrum is from decays occurring in the Ge(Li) room.

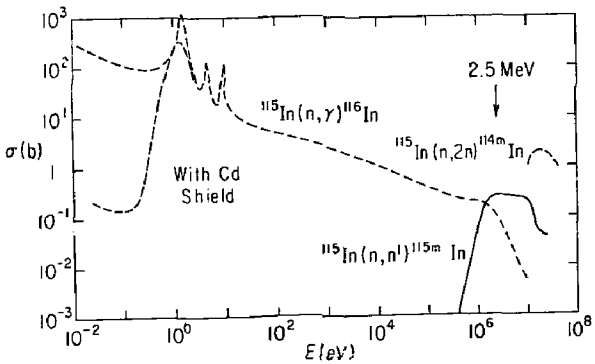

(PPPL-806098)

Fig. 2 The cross sections for neutron activation of Indium.

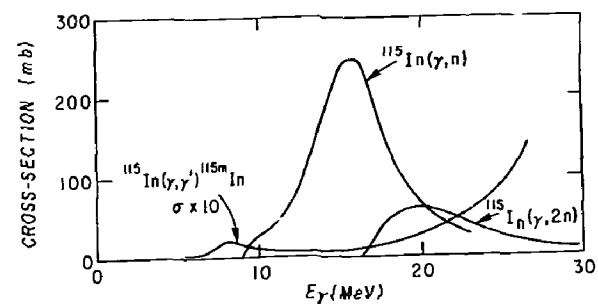

(PPPL-806100)

Fig. 3. The cross sections for photon activation of Indium.

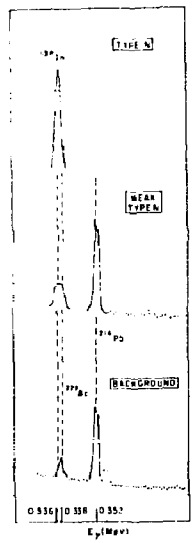

(PPPL-806094)

Fig. 4. High resolution Ge(Li) spectrum in the vicinity of the 0.336 MeV ^{115m}In line. The type N spectrum shows the strong ^{115m}In line. The background spectrum shows only the interfering 0.338 ^{228}Ac line. Weak type N spectra are a combination of ^{115m}In and ^{228}Ac lines.

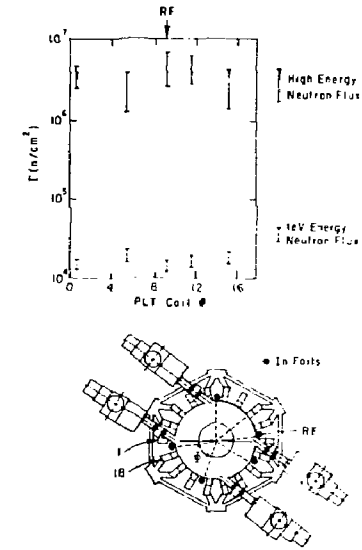

(PPPL-806093)

Fig. 5. a) Schematic diagram of PLT indicating the Indium foil positions for a toroidal scan of local neutron flux. b) 2.5 MeV and 1 eV local neutron fluxes indicating toroidally symmetric neutron emission. The neutron emission was thermonuclear resulting from the bulk deuteron heating from an ICRF heated ^{3}He tail distribution.

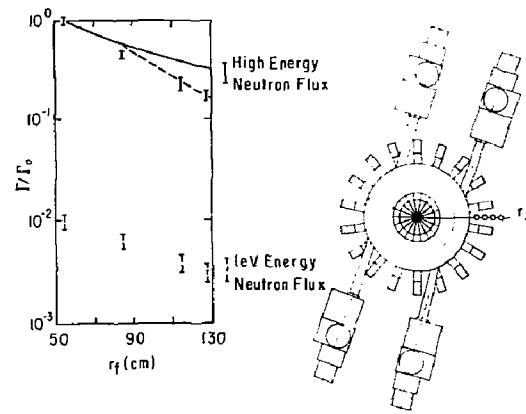

(PPPL-806105)

Fig. 6. a) Schematic diagram of PLT indicating the Indium foil locations for a scan of local versus distance away from the plasma r_f. b) 2.5 MeV and 1 eV local neutron fluxes versus r_f. The solid line is the 2.5 MeV intensity expected from an unshielded toroidal neutron source. The dashed line takes into account the shielding by the Copper toroidal magnetic field coils.

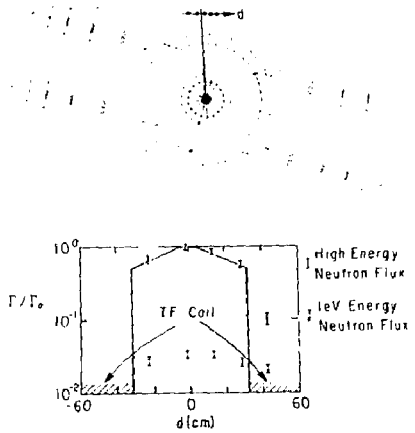

(PPPL-806104)

Fig. 7. a) Schematic diagram of PLT indicating the Indium foil locations for a scan of local flux behind the toroidal magnetic field coils. b) 2.5 MeV and 1 eV local neutron fluxes in the gap between the toroidal magnetic field coils. The solid line is the 2.5 MeV intensity expected from a toroidal neutron source shielded by the toroidal field coils.

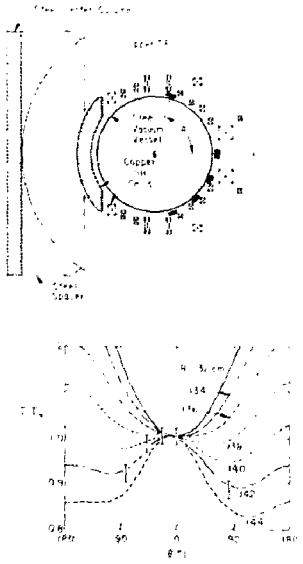

(PPPL-806097)

Fig. 8. a) Schematic diagram of PLT indicating the Indium foil positions for a poloidal scan of the local neutron flux. b) Poloidal symmetry of the local 2.5 MeV local neutron flux. The lines indicate the expected poloidal symmetry for toroids of major radii 132→144 cm. The PLT vessel major radius is 134 cm while the major radius of the neutron emission is shifted 8 cm outwards. The neutron emission is beam-induced resulting from 2Co + 1CTR $D^0 \rightarrow H^+$ neutral beam injection.

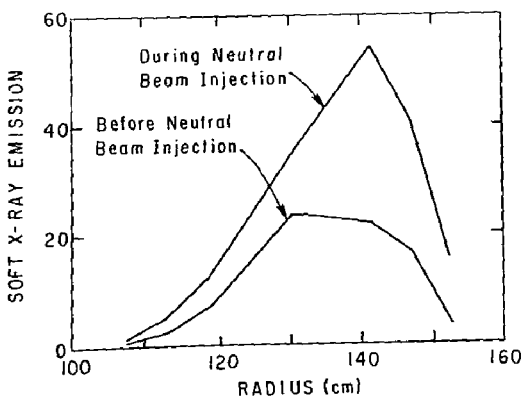

(PPPL-806095)

Fig. 9. The vertical profile of the soft x-ray emission from PLT discharges similar to those for Fig. 8b. The soft x-ray emission also has an outward shift comparable to the neutron emission.

(PPPL-806103)

Fig. 10. Schematic diagram of the toroidal geometry.

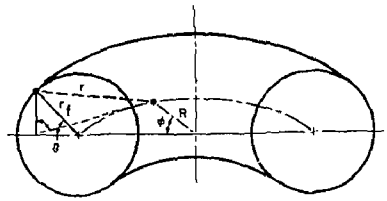

(PPPL-806101)

Fig. 11. The average neutron emission for 109 PLT discharges distributed over 6 hours featuring $D^0 \rightarrow H^+$ neutral beam injection. The saturation of activation is equivalent to one discharge having a 3.7×10^{13} neutron yield at the time of the last shot.

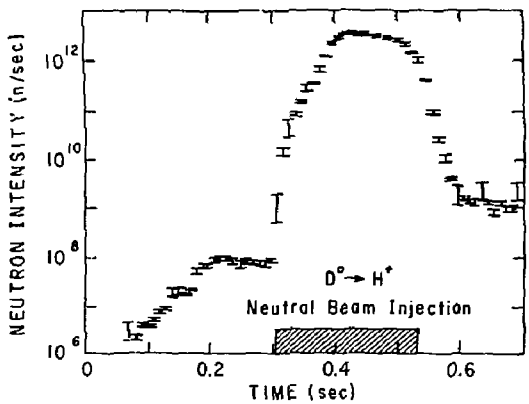

(PPPL-806076)

Fig. 12. The PLT neutron spectrum measured inside a neutron collimator situated about 5 m from the PLT plasma and viewing tangentially. The virgin neutron spectrum is expected to be about 150 keV wide, centered at 2.45 MeV. The remaining neutrons have degraded energies due to scattering.